Supporting Information

Trimetallic conductivitive metal-organic frameworks as precatalysts for the oxygen evolution reaction with enhanced activity

Xiaofei Shi[#], Rui Hua[#], Yulong Xu, Tong Liu, and Guang Lu[*]

Institute of Functional Nano & Soft Materials (FUNSOM), Jiangsu Key Laboratory for Carbon-Based Functional Materials & Devices, Soochow University, 199 Ren'ai Road, Suzhou, 215123, Jiangsu, PR China

Corresponding Author

*glu@suda.edu.cn

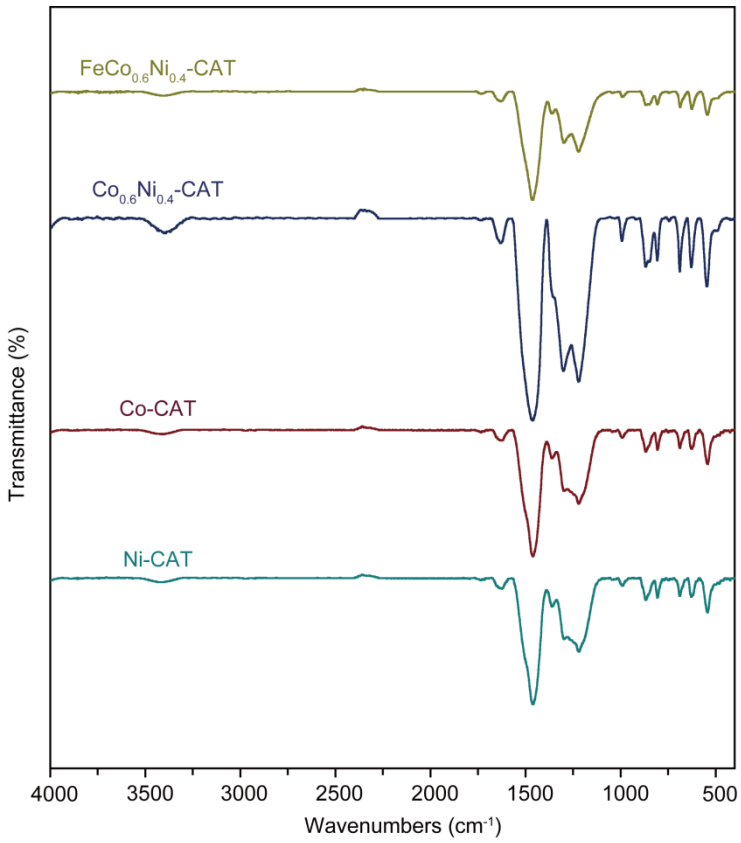

Figure S1. FT-IR spectra of $FeCo_{0.6}Ni_{0.4}$-CAT, $Co_{0.6}Ni_{0.4}$-CAT, Co-CAT, and Ni-CAT.

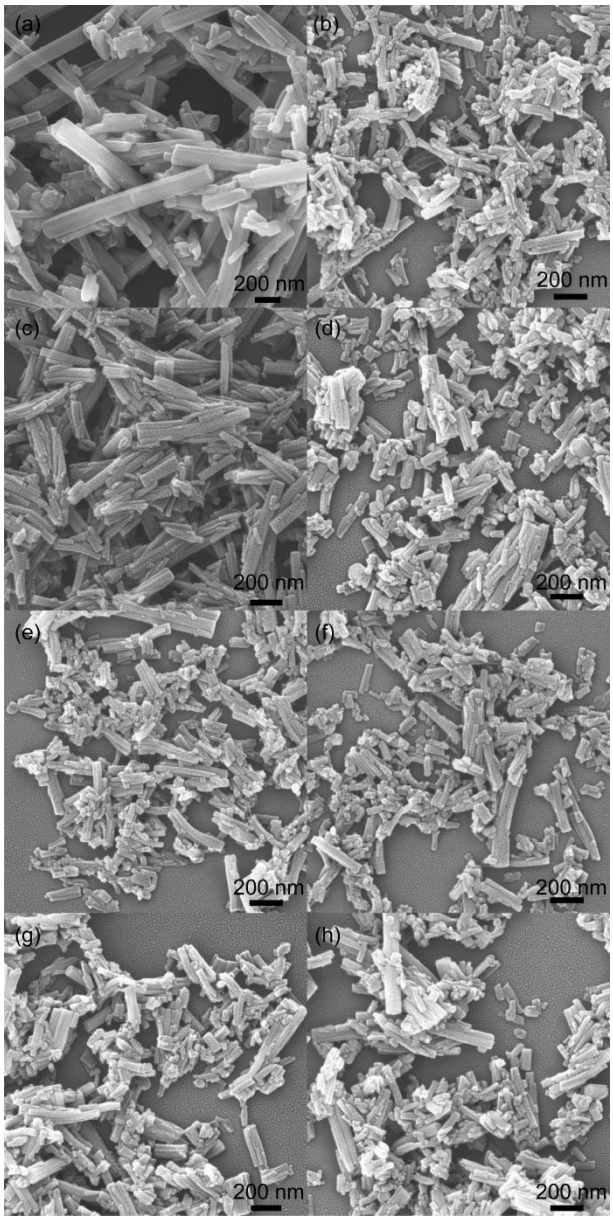

Figure S2. SEM images of a) Co-CAT, b) FeCo-CAT, c) Ni-CAT, d) FeNi-CAT, e) $Co_{0.8}Ni_{0.2}$-CAT, f) $FeCo_{0.8}Ni_{0.2}$-CAT, g) $Co_{0.4}Ni_{0.6}$-CAT, and h) $FeCo_{0.4}Ni_{0.6}$-CAT, respectively.

Table S1. ICP analysis of $FeCo_xNi_{1-x}$-CATs obtained in 1.0 mM $Fe(OAc)_2$ methanol solition at 25 ℃.

Sample	Atom contents (wt %)			Atom ratios in the total atom contents of Co and Ni		
	Co	Ni	Fe	Co	Ni	Fe/(Co+Ni)
FeCo-CAT	17.48	—	5.37	1.0	0	0.31
$FeCo_{0.8}Ni_{0.2}$-CAT	13.65	3.70	5.45	0.79	0.21	0.31
$FeCo_{0.6}Ni_{0.4}$-CAT	10.15	7.11	5.49	0.59	0.41	0.32
$FeCo_{0.4}Ni_{0.6}$-CAT	7.18	9.97	5.46	0.42	0.58	0.32
FeNi-CAT	—	17.93	5.42	0	1.0	0.30

Table S2. ICP analysis of $FeCo_{0.6}Ni_{0.4}$-CATs obtained in different concentrations of $Fe(OAc)_2$ methanolic solution at 25 ℃.

Concentration of $Fe(OAc)_2$ (mmol)	Atom contents (wt %)			Atom ratios in the total atom contents of Co and Ni		
	Co	Ni	Fe	Co	Ni	Fe/(Co+Ni)
0.25	12.76	8.61	1.27	0.60	0.40	0.06
0.5	11.54	8.07	2.94	0.59	0.41	0.15
1.0	10.15	7.11	5.49	0.59	0.41	0.32
2.0	9.01	6.42	7.52	0.58	0.42	0.49

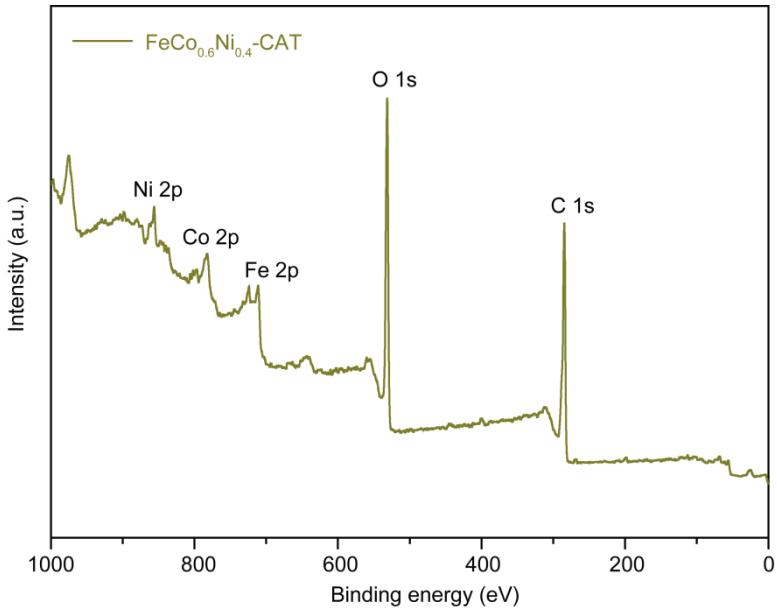

Figure S3. Full XPS spectrum of $FeCo_{0.6}Ni_{0.4}$-CAT.

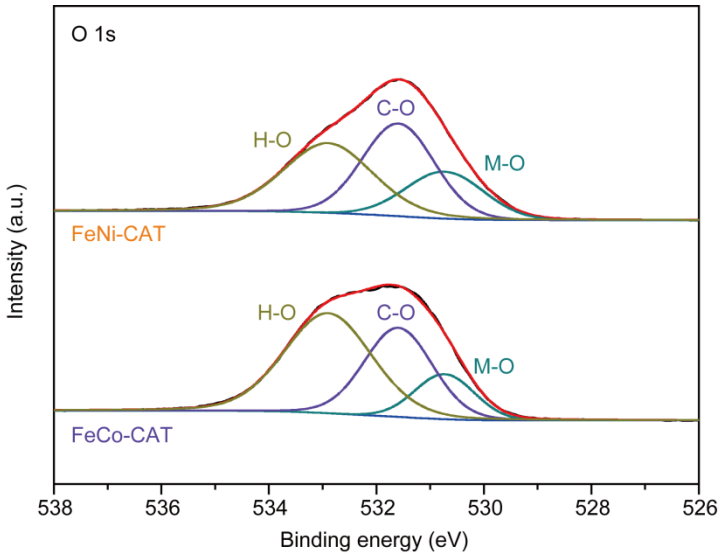

Figure S4. High resolution XPS spectra of O 1s of FeNi-CAT and FeCo-CAT.

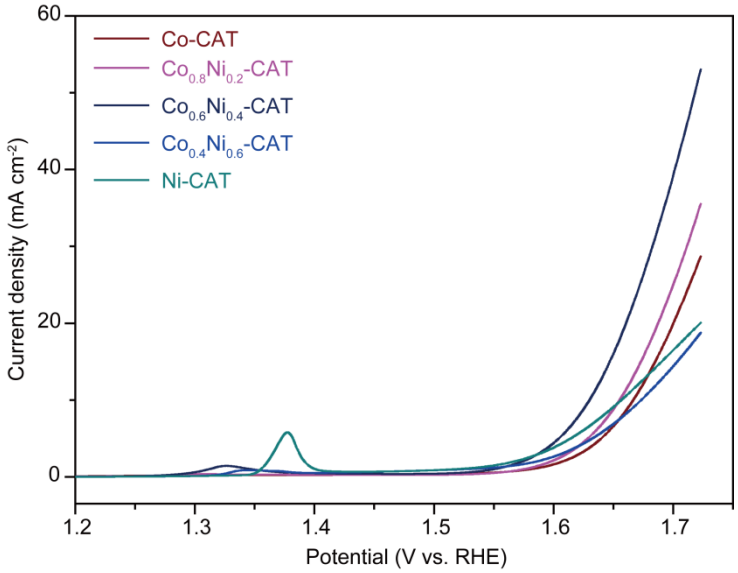

Figure S5. LSV curves of Co_xNi_{1-x}-CATs (x= 1.0, 0.8, 0.6, 0.4, 0).

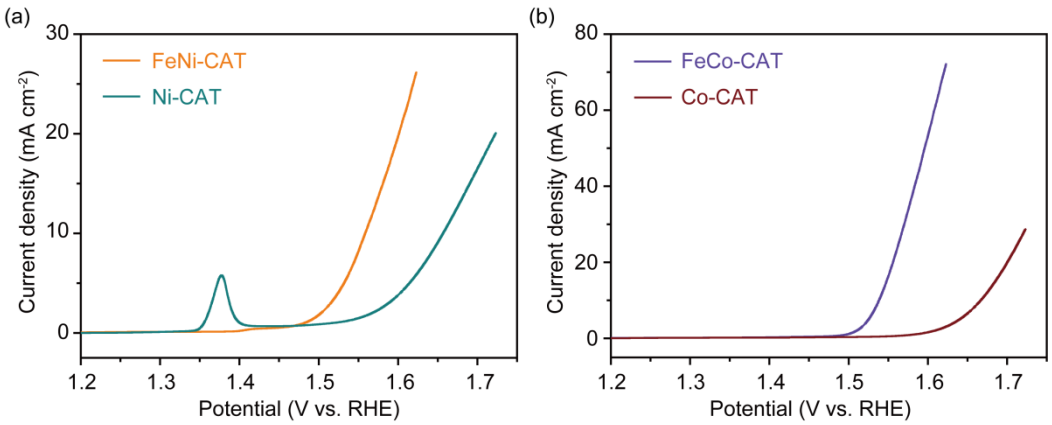

Figure S6. LSV curves of a) FeNi-CAT and Ni-CAT, and b) FeCo-CAT and Co-CAT.

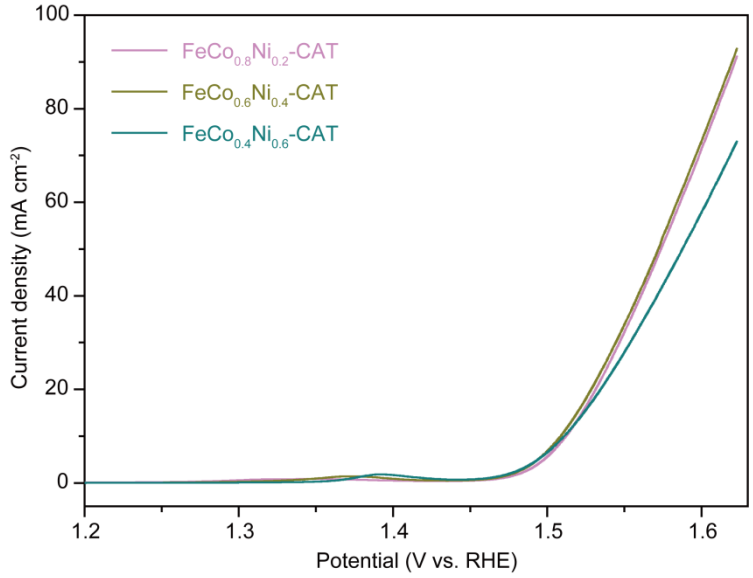

Figure S7. LSV curves of $FeCo_{0.8}Ni_{0.2}$-CAT, $FeCo_{0.6}Ni_{0.4}$-CAT, and $FeCo_{0.4}Ni_{0.6}$-CAT.

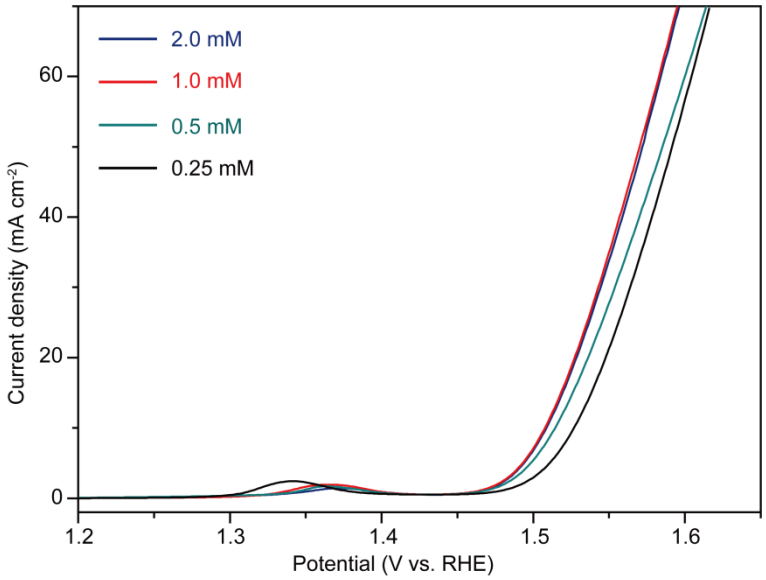

Figure S8. LSV curves of $FeCo_{0.6}Ni_{0.4}$-CAT obtained via cation-exchange in 0.025, 0.05, 0.1, 0.2 mM $Fe(OAc)_2$ solutions, respectively.

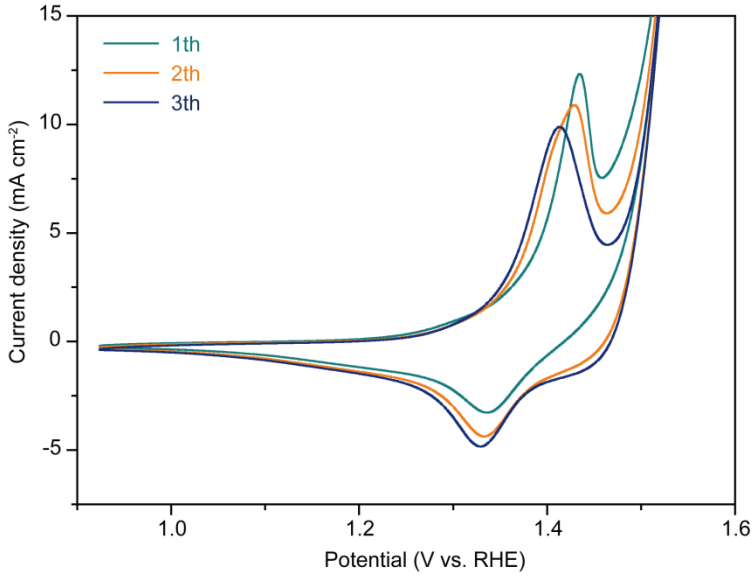

Figure S9. The early three CV cycles measured in the potential range of 0.924~1.624 V (vs. RHE) with a scan rate of 10 mV s^{-1} for $FeCo_{0.6}Ni_{0.4}$-CAT during activation process.

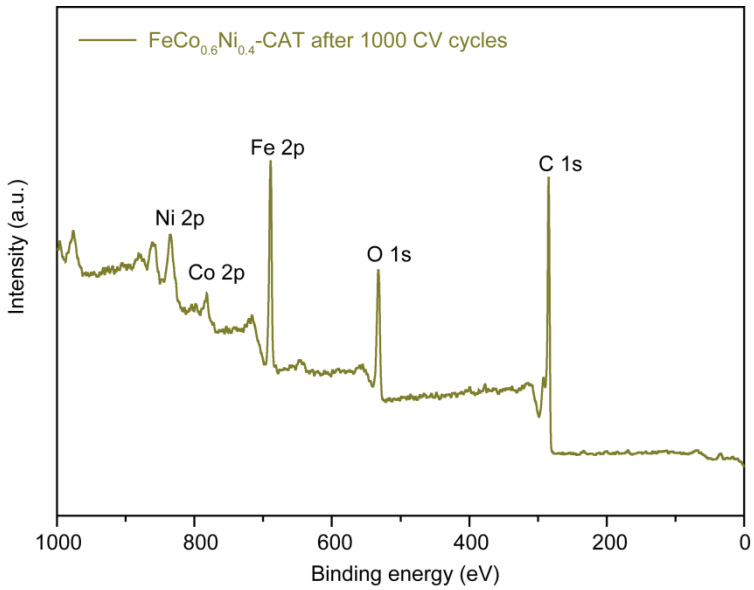

Figure S10. Full XPS spectrum of $FeCo_{0.6}Ni_{0.4}$-CAT after 1000 cycles of CV scans.

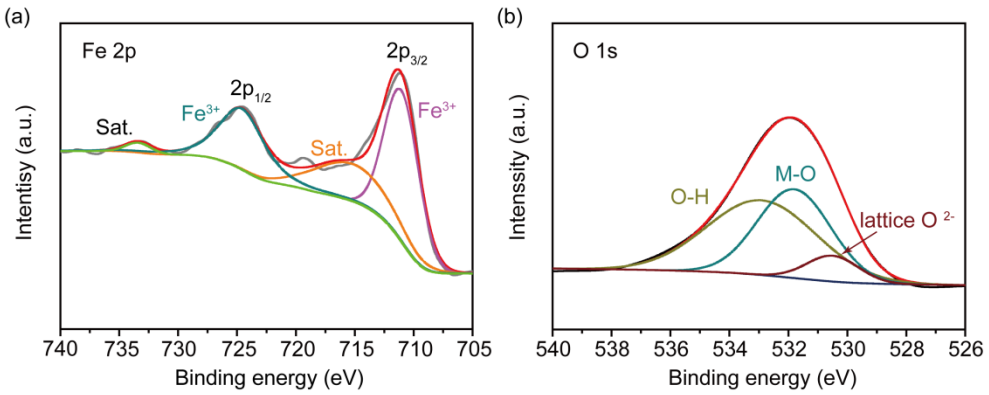

Figure 11. High resolution XPS spectra of a) Fe 2p and b) O 1s of $FeCo_{0.6}Ni_{0.4}$-CAT after 1000 cycles of CV scans.

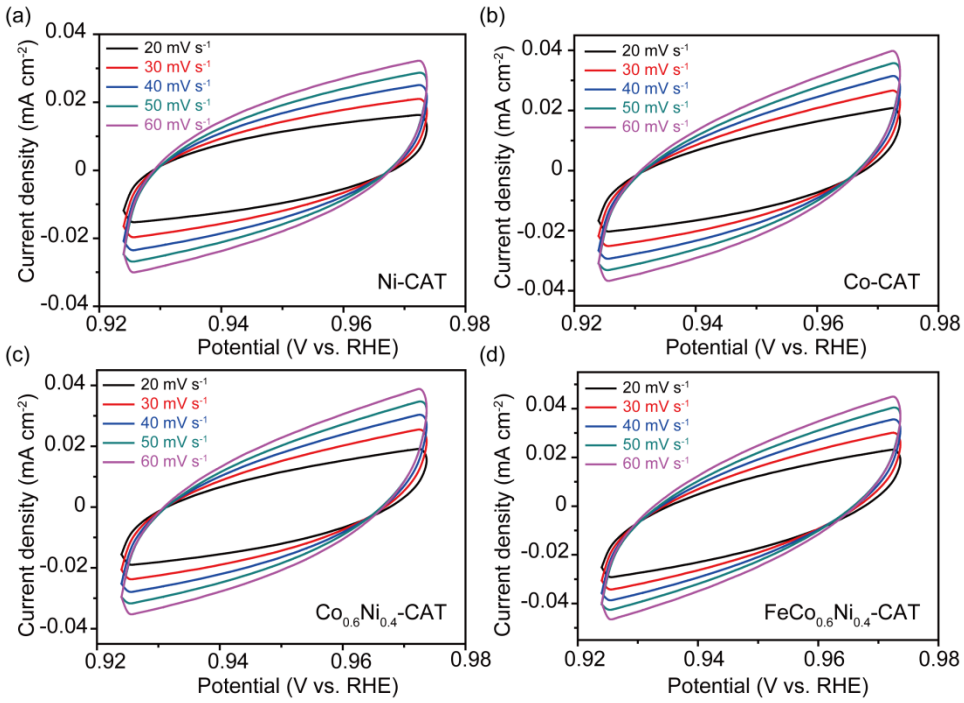

Figure S12. CV curves measured in a potential range of 0.924~0.974 V (vs. RHE) with the scan rates of 20, 30, 40, 50, and 60 mV s^{-1} for a) Ni-CAT, b) Co-CAT, c) $Co_{0.6}Ni_{0.4}$-CAT, and d) $FeCo_{0.6}Ni_{0.4}$-CAT, respectively.

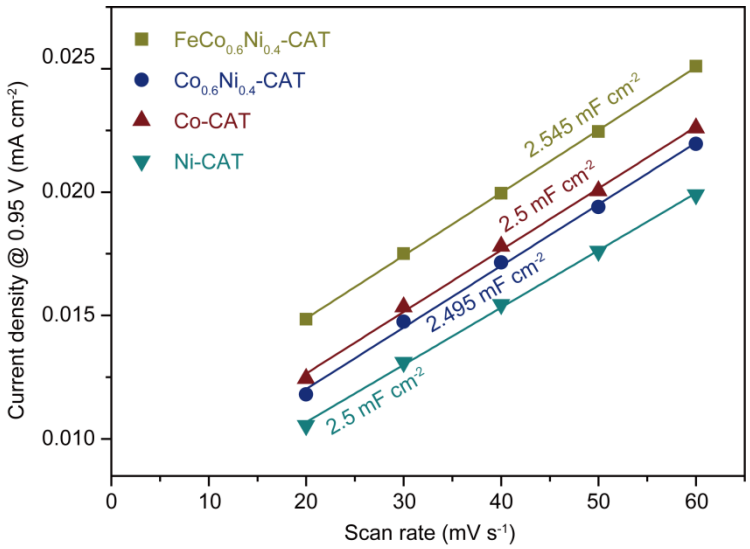

Figure S13. Linear plot of ΔJ ((Ja - Jc)/2 at 0.95 V vs. RHE) of CVs measured at different scan rates in a non-Faradaic region against scan rate for Ni-CAT, Co-CAT, $Co_{0.6}Ni_{0.4}$-CAT, and $FeCo_{0.6}Ni_{0.4}$-CAT.

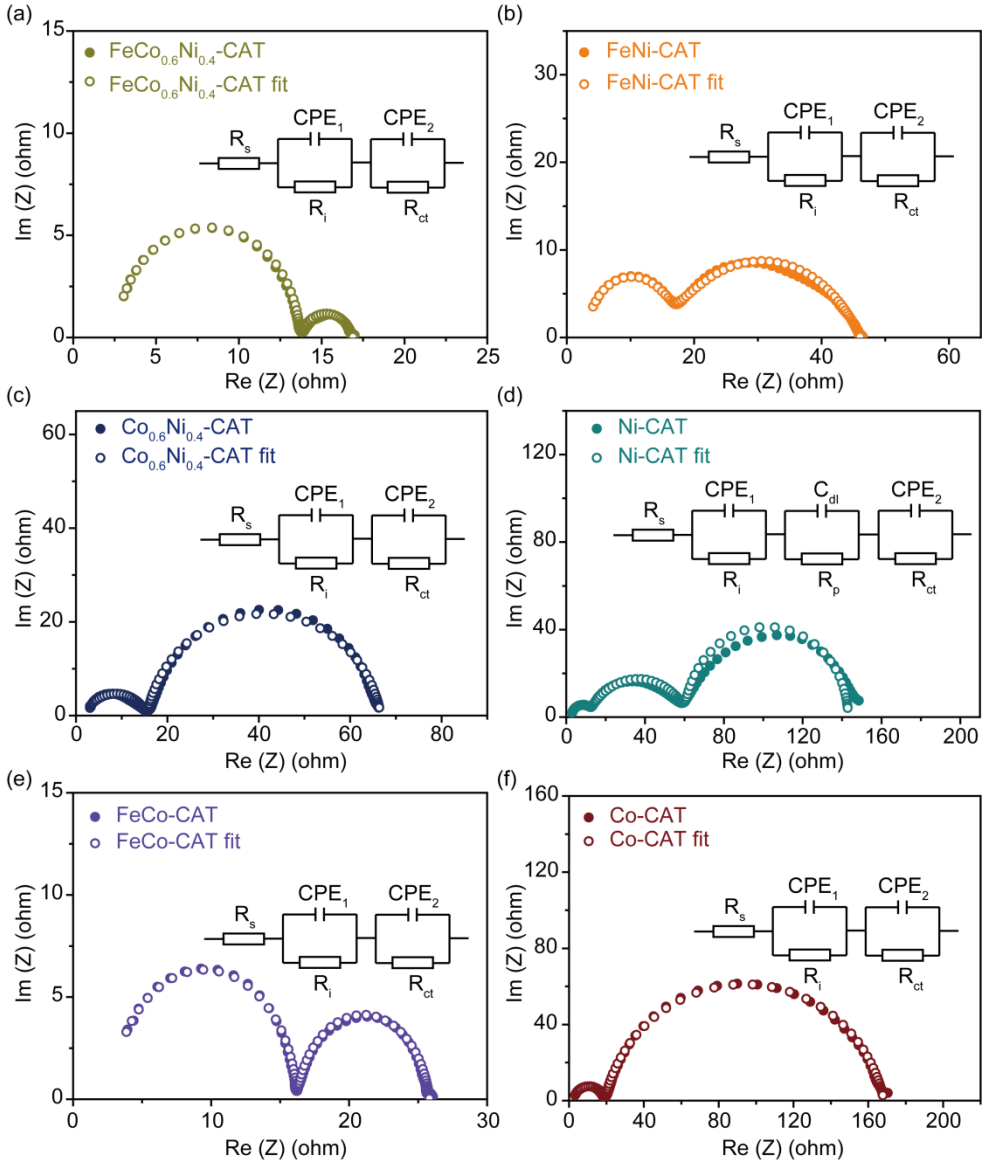

Figure S14. Nyquist plots recorded at 1.63 V (vs. RHE) and corresponding fit plots for a) $Fe_{0.6}Co_{0.4}$-CAT, b) FeNi-CAT, c) $Co_{0.6}Ni_{0.4}$-CAT, d) FeCo-CAT, and f) Co-CAT. Inset: equivalent circuit models.

Table S3. Different fit resistances and their errors corresponding to the equivalent circuit for $FeCo_{0.6}Ni_{0.4}$-CAT, FeNi-CAT, $Co_{0.6}Ni_{0.4}$-CAT, Ni-CAT, FeCo-CAT, and Co-CAT.

Sample	R_s (Ω)	Errors of R_s (%)	R_i (Ω)	Errors of R_i (%)	R_{ct} (Ω)	Errors of R_{ct} (%)	R_p (Ω)	Errors of R_p (%)
$FeCo_{0.6}Ni_{0.4}$-CAT	2.6	0.9	11.1	0.3	3.2	1.3		
FeNi-CAT	3.1	2.5	12.4	1.5	30.6	0.7		
$Co_{0.6}Ni_{0.4}$-CAT	1.9	8.4	13.7	1.74	51.1	1.6		
Ni-CAT	2.6	4.0	8.9	4.0	81.9	1.7	49.7	1.5
FeCo-CAT	2.8	1.7	13.4	0.5	9.6	0.6		
Co-CAT	2.3	4.5	16.9	1.0	149.1	0.7		

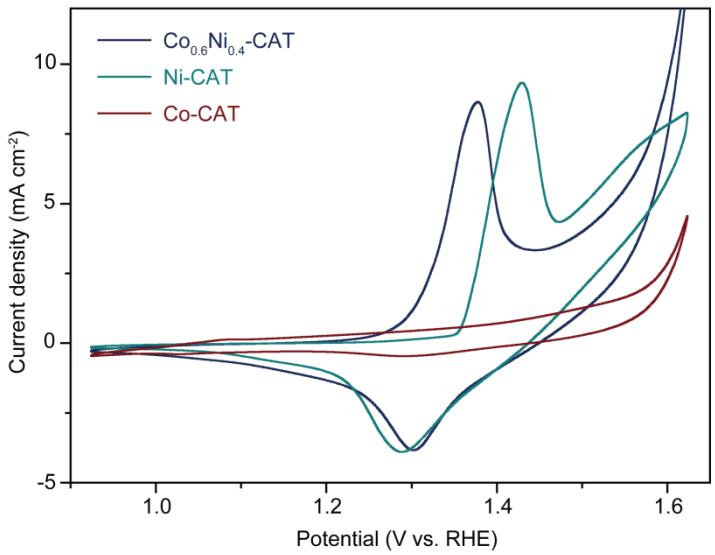

Figure S15. CV curves measured in the potential range of 0.924~1.426 V (vs. RHE) with a scan rate of 10 mV s^{-1} for $Co_{0.6}Ni_{0.4}$-CAT, Ni-CAT, and Co-CAT.

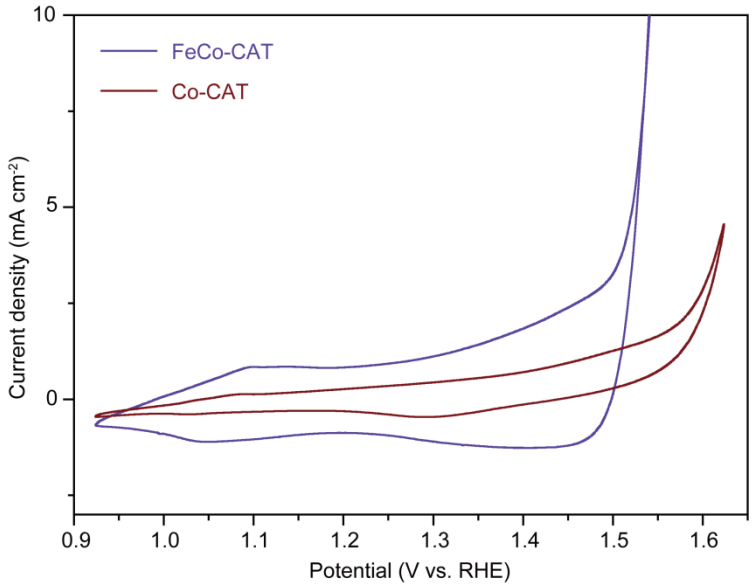

Figure S16. CV curves measured in the potential range of 0.924~1.426 V (vs. RHE) with a scan rate of 10 mV s^{-1} for Co-CAT and FeCo-CAT.